Catalysis Communications 103 (2018) 29–33

Contents lists available at ScienceDirect

Catalysis Communications

journal homepage: www.elsevier.com/locate/catcom

Short communication

The roles of surface oxygen vacancy over $Mg_4Ta_2O_{9\text{-}x}$ photocatalyst in enhancing visible-light photocatalytic hydrogen evolution performance

Entian Cui[a], Qiangqiang Meng[a], Chengyan Ge[b], Guiyun Yu[b], Guihua Hou[a], Ning Xu[c], Feng Zhang[a], Yuqi Wu[d,*]

[a] Key Laboratory for Advanced Technology in Environmental Protection of Jiangsu Province, Yancheng Institute of Technology, Yancheng 224051, PR China
[b] School of chemistry and chemical engineering, Yancheng Institute of Technology, Yancheng 224051, PR China
[c] Physics Department, Yancheng Institute of Technology, Yancheng 224051, PR China
[d] State Key Laboratory for Oxo Synthesis and Selective Oxidation, Lanzhou Institute of Chemical Physics, Chinese Academy of Science, Lanzhou 730000, PR China

ARTICLE INFO

Keywords:
Photocatalysis
Oxygen vacancy
Defect level band
$Mg_4Ta_2O_{9\text{-}x}$
Hydrogen evolution

ABSTRACT

Extending the light absorption range of wide-band-gap semiconductor oxides is crucial to the effective solar-hydrogen energy conversion. Here, we introduced surface oxygen vacancies into $Mg_4Ta_2O_9$ and constructed a narrow band-gap $Mg_4Ta_2O_{9\text{-}x}$ photocatalyst by a simple low temperature reduction method. The as-synthesized $Mg_4Ta_2O_{9\text{-}x}$ exhibits a significantly extended absorption edge in visible light range, which originates from the intermediate defect level band and electronic states created by introducing surface oxygen vacancy. With the same Pt loaded content (0.5 wt%), the Pt-loaded $Mg_4Ta_2O_{9\text{-}x}$ exhibits the excellent photocatalytic stability and higher hydrogen evolution activity (4.42 μmol·h^{-1}) than the Pt-loaded $Mg_4Ta_2O_9$ (0.14 μmol·h^{-1}) under visible light irradiation.

1. Introduction

Photocatalytic water splitting has been emerging as a promising and environmental friendly way for hydrogen production. Owing to the suitable band and special lattice structures, the layered perovskite type materials containing octahedral TaO_6 are considered to be suitable candidates for water splitting, and the photo-generated electron-hole pairs can be mobilized, transferred and separated easily [1–4]. Because of the wide band gap (ca. 3.0–4.0 eV), the tantalum-based compounds are only photoactive under UV light, and the efficiency for solar energy utilization is low [5]. Many strategies, including transition metals and/or anion doping, have been developed by tuning their band gap to achieve the visible light response [6–8]. Even so, there are still some problems to be solved, including: (1) nitrogen-doped tunneled oxides usually show weak absorption in the visible region due to the low content of nitrogen incorporated; (2) the size of tunneled oxides particles is quasi micrometer-sized for the high calcination temperature; (3) the dopants usually act as electron-hole recombination centers reducing the photocatalytic efficiency; (4) the doped materials suffer thermal instability [9–10]. Another efficient strategy is to introduce oxygen vacancies [11–19]. Recent reports showed that the intrinsic metal oxides with oxygen vacancies can absorb visible light and display excellent visible light photocatalytic activity [15–18]. The oxygen vacancies have been believed to affect the electron-hole recombination process, and thus cause changes in chemical reaction rates [19]. In additions, loading appropriate cocatalyst, such as Pt or NiO species, is important to enhancing photocatalytic activity for hydrogen production. For examples, Lianzhou Wang' group has reported photocatalytic hydrogen production on Pt-loaded graphene- $Sr_2Ta_2O_{7\text{-}x}N_x$ photocatalyst under simulated solar light irradiation [4]. The loaded Pt species only was used as the standard cocatalyst by providing active sites for hydrogen production. Akihiko Kudo' group reported that the $Sr_2Ta_2O_7$ and $Sr_2Nb_2O_7$ with similar layered perovskite structure showed activities for water splitting into H_2 and O_2 in pure water without any additives under UV irradiation [6]. They found the $Sr_2Ta_2O_7$ gave H_2 and O_2 from pure water under UV irradiation even in the absence of a cocatalyst, and the activity of $Sr_2Ta_2O_7$ was much increased by loading NiO as a cocatalyst even without pretreatment (The quantum yield of the NiO/$Sr_2Ta_2O_7$ photocatalyst was 12% at 270 nm). They also found the native $Sr_2Nb_2O_7$ did not possess the activity, and the high activity was obtained for the $Sr_2Nb_2O_7$ photocatalyst when NiO was loaded and pretreated.

In this study, we demonstrated for the first time that the light-harvesting ability and the photo-generated electron-hole pair separation efficiency of $Mg_4Ta_2O_9$ can be improved through inducing oxygen vacancies. Oxygen deficient $Mg_4Ta_2O_{9\text{-}x}$ has showed a remarkable red

---

* Corresponding author.
E-mail address: wuyuqicas@163.com (Y. Wu).

http://dx.doi.org/10.1016/j.catcom.2017.09.018
Received 7 July 2017; Received in revised form 5 September 2017; Accepted 19 September 2017

shift of about 290 nm in light absorption edge, and exhibited 22 times higher photocatalytic hydrogen evolution activity than the untreated $Mg_4Ta_2O_9$ and the outstanding cycling performance under visible light irradiation as well.

2. Experimental

All chemical reagents in our experiments were purchased from J & K Scientific Ltd. and used without further purification, and the preparation, characterization, and computational of $Mg4Ta_2O_9$ and $Mg4Ta_2O_{9-x}$ Sample $Mg_4Ta_2O_{9-x}$ is presented in the Supporting Information Section I in details [7,20–23].

3. Results and discussion

The crystal structures of $Mg_4Ta_2O_9$ and $Mg_4Ta_2O_{9-x}$ particles were investigated by X-ray powder diffraction (XRD) patterns (Fig. S1A). A single phase of $Mg_4Ta_2O_9$ with high crystallinity was confirmed. A similar XRD profile was also observed for the sample $Mg_4Ta_2O_{9-x}$, demonstrating that the effect of reduction treatment on the crystal structure was negligent. Besides the crystalline structure, the similar surface areas (about $1.2\,m^2{\cdot}g^{-1}$ for $Mg_4Ta_2O_9$ and $1.2\,m^2{\cdot}g^{-1}$ for $Mg_4Ta_2O_{9-x}$, Fig. S1B), morphology, and the particle sizes (estimated to be ca. 100–400 nm) were also identified for sample $Mg_4Ta_2O_9$ and $Mg_4Ta_2O_{9-x}$ (Fig. S2A and B). All these results integrally revealed that the Mg-thermal reduction treatment had no remarkable effect on the size, structure, and morphology of sample $Mg_4Ta_2O_9$.

The surface chemical state of sample $Mg_4Ta_2O_9$ and $Mg_4Ta_2O_{9-x}$ was examined with X-ray photoelectron spectroscopy (XPS). The Ta4p XPS spectra of the white $Mg_4Ta_2O_9$ were basically consistent with that of the black $Mg_4Ta_2O_{9-x}$ sample, which indicated that the bonding environment of Ta atoms before and after Mg-thermal treatment had no obvious changes (Fig. S3). However, the O 1s XPS spectra presented a dramatic difference between sample $Mg_4Ta_2O_9$ and $Mg_4Ta_2O_{9-x}$ (Fig. 1). For sample $Mg_4Ta_2O_9$, the O1s peak can be resolved into three peaks at about 529.6, 530.0, and 531.1 eV, and attributed to Mg—O (O—I), Ta—O (O-II), and Ta—OH species (O—III), respectively. These two types of oxygen atoms in TaO_6 unit cell differ in their proximity to Mg atoms, O—I being closer and O-II farther [20], which resulted in two peaks with different binding energy. For $Mg_4Ta_2O_{9-x}$, the O1s peak can also be resolved into three peaks with the binding energies at 529.6, 530.2, and 531.0 eV, respectively. Compared with $Mg_4Ta_2O_9$, the binding energy of Ta—O (O—II) was changed. What's more, the relative area ratio of O—II to O—I in $Mg_4Ta_2O_{9-x}$ was lower than that in $Mg_4Ta_2O_9$, indicating that the O—II was the vacancy sites, which was consistent with the theoretical calculation results reported in a previous study [20]. In addition, the atom ratios of Ta to O were about 1:4.3 and 1:3.8 for sample $Mg_4Ta_2O_9$ and $Mg_4Ta_2O_{9-x}$, respectively, which also proved that oxygen vacancies had been formed obviously after Mg-thermal treatment.

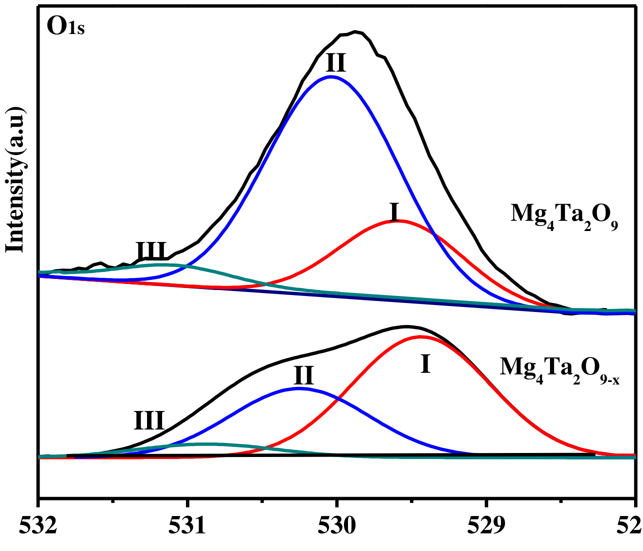

Fig. 1. O1s XPS spectra of $Mg_4Ta_2O_9$ and $Mg_4Ta_2O_{9-x}$ samples.

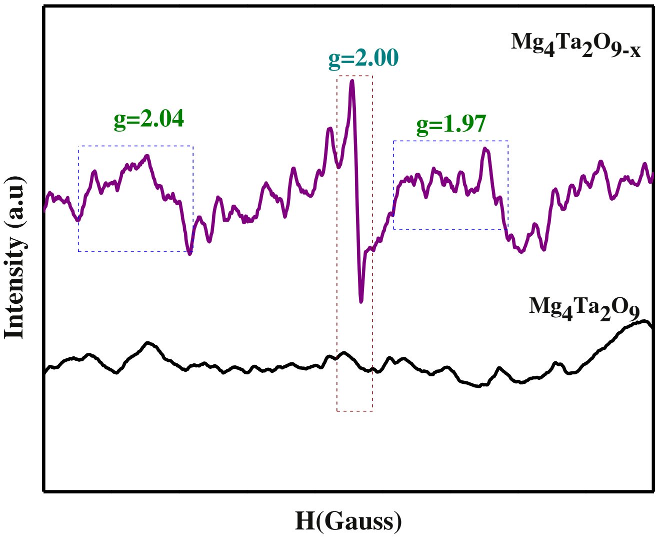

Fig. 2. Electron spin resonance of sample $Mg_4Ta_2O_9$ and $Mg_4Ta_2O_{9-x}$.

The oxygen vacancies were indeed introduced into $Mg_4Ta_2O_{9-x}$, as evidenced by electron spin resonance (EPR) spectra (Fig. 2). The sample $Mg_4Ta_2O_{9-x}$ exhibited a strong EPR signal at about $g \sim 2.00$, which was a typical signal of oxygen vacancies [24,25]. In addition, two other peaks at $g \sim 2.04$ corresponded to chemisorbed oxygen O_2^-[26,27] and $g \sim 1.97$ was assigned to shallow donors or singly ionized oxygen vacancy (Vo^+) [27,28]. These indicated that other defects may be produced besides those surface oxygen vacancies mainly generated. Photoluminescence spectrum (PL) is an effective way to study the electronic structure, optical and photochemical properties of semiconductor materials [29,30]. An obvious difference in PL curves of sample $Mg_4Ta_2O_9$ and $Mg_4Ta_2O_{9-x}$ was observed (Fig. S4). For sample $Mg_4Ta_2O_9$, only a broad violet peak at 325–350 nm was observed, and originated from the exciton recombination corresponding to the near band edge exciton emission of the wide band gap of $Mg_4Ta_2O_9$[31]. While for sample $Mg_4Ta_2O_{9-x}$, five emission bands, including a violet emission at around 325–350 nm (peak 1), a blue band at about 420–430 nm (peak 2), and three green bands at about 480 (peak 3), 525 (peak 4), and 588 nm (peak 5) were observed. The wavelengths of peak 2 to 5 were in visible light range, which was considered to be related to oxygen vacancies [32]. Compared with $Mg_4Ta_2O_9$, a slight blue shift for $Mg_4Ta_2O_{9-x}$ was observed, which further indicated the existing of oxygen vacancies might decrease the average atomic mass and cause mass fluctuations at the oxygen positions, resulting in a shift in the peak position towards lower wavenumber values [33]. It should reinforce the point that the wavelength of peak 5 was 570–610 nm, which corresponded to the valence band edge of $Mg_4Ta_2O_{9-x,}$ as evidenced by the UV–Vis diffuse reflectance spectra (DRS) showed in Fig. 3. A significantly extended visible light absorption was found for the sample $Mg_4Ta_2O_{9-x}$. The band gap of $Mg_4Ta_2O_{9-x}$ was estimated to be ca. 2.10 eV from the Kubelka–Munk function, which was much narrower than that of $Mg_4Ta_2O_9$ (4.12 eV). An abrupt change in the DRS spectrogram at approximately 2.02 eV suggested that the optical gap of the black $Mg_4Ta_2O_{9-x}$ was substantially narrowed by intraband transitions [15], which was directly related to the formation of defect level band resulted from the introduction of oxygen vacancies.